

Supplementary Materials

Cooperative assembly and misfolding of CFTR domains *in vivo*

Kai Du and Gergely L. Lukacs

Dept. Physiology, McGill Univ., Montreal, QC, Canada, H3G 1Y6

Supplementary Results

Processing defect of two and three-domain combinations of CFTR

Transient co-expression of cytosolic domains in various configurations and combinations (CD4T-N1* + CD4T-N2, CD4T-N1* + R-IiT, CD4T-N2 + R-IiT, CD4T-N1R + CD4TN2, CD4T-N1* + CD4T-N2 + R-IiT and CD4T-N1R) failed to promote significant processing, measured by immunoblotting and cell surface anti-CD4 (Fig.S4a and Fig.3a) or anti-Ii Ab binding (Fig.S4b). Similar data were obtained with the CD4T-N1 constructs (data not shown).

Multidomain fragments, containing the MSD1 or MSD2 were largely trapped in the ER. Neither EGFP-MSD1-NBD1 (M1-N1 or M1-N1*) nor M1-N1-R domain combination restored processing and cell surface expression (Supplemental Fig.S4d-e). Likewise, processing and cell surface accumulation of M2-N2, R-M2-N2 and R-M2 (or R*-M2-N2 and R*-M2), as well as the combination of M2 with M1, M1N1 or CD4T-N1 were undetectable by immunolocalization, electrophoretic mobility shift and cell surface Ab-binding (Fig.1a-b, Supplemental Fig. S4a-b, f-g and Fig.5). N1RM2 was also trapped in the ER (see Fig.6a).

Supplemental Figure Legends

Supplemental Figure 1. Functional and biochemical complementation of split CFTRs.

a) Schematic representation of the N- and C-terminal fragments of the split CFTR variants. The domain boundaries are defined in the Supplemental Table. **b)** Cotransfection of the M1 and N1RM2N2 domain conferred PKA-stimulated halide conductance to plasma membrane of COS7 cells, measured by the iodide efflux assay. PKA was activated at time 0. Wt CFTR expressing and mock-transfected cells were used as positive and negative control, respectively. **c)** Physical association of the indicated N- (M1N1 and M1) and C-terminal (RM2N2 and N1RM2N2) fragments of CFTR. COS7 cells, expressing the indicated

constructs, were lysed and the CFTR C-terminal half was precipitated with a polyclonal anti-CFTR Ab. Lysates and immunoprecipitates were probed with anti-HA and MM13-4 (anti-N-terminus) Ab. Note that complex-glycosylated MSD2 (M2) containing fragments were only observed in the presence of the complementing N-terminal fragment.

Supplemental Figure 2. Expression of CD4T-CFTR chimeras in BHK cells.

BHK cells were transiently transfected with the indicated constructs. N1ΔF, NBD1-ΔF508; N2K, NBD2-1303K. **a)** Cells were lysed and equal amounts of proteins were separated by SDS-PAGE for immunoblotting with polyclonal anti-CD4 Ab. **b)** Cell surface density of CD4T-CFTR chimeras. The cell surface density was measured by the immunoperoxidase assay as described in Methods. Mean ± SEM, n=3-4. **c)** Indirect immunostaining of the chimeras with anti-CD4 Ab was described in Fig. 2f. The plasma membrane and the Er was stained with Alexa594-WGA and anti-calnexin Ab (CNX), respectively.

Supplemental Figure 3. Probing the 4D CFTR conformational change by limited proteolysis.

Isolated microsomes expressing 4D or wt CFTR were subjected to limited proteolysis at the indicated chymotrypsin concentration on ice for 15 min. The proteolytic digestion patterns of CFTR were analyzed by immunoblotting using the N-terminal (MM13-4), NBD1 (660) and NBD2 (M3A7) specific antibody (*top panels*). The protease resistance of the full-length CFTR (*left-bottom panel*) as well as the NBD1 and NBD2 containing proteolytic fragments were measured by the abundance of the respective polypeptide fragments by densitometric analysis and expressed as the percentage of the maximum (*bottom panels*).

Supplemental Figure 4. Processing defect of domain combinations of CFTR.

a-b) The CD4 and Ii chimeras were transiently expressed in COS7 cells. The plasma membrane and cellular expression levels were determined by the immunoperoxidase assay and immunoblotting, respectively, with anti-CD4 and anti-Ii primary Abs. **c)** Expression

pattern of the various MSD2s in transiently transfected COS7 cells with the indicated domain boundaries. Immunoblotting was performed with anti-HA Ab. **d)** Expression of MSD1 containing domain combinations. EGFP was fused to the N-terminus of M1, M1N1 and M1N1R, expressed in COS7 cells and analyzed by immunoblotting with the L12B4 anti-CFTR Ab. **e)** Colocalization of EGFP-M1N1 with Alexa594-WGA and CNX was performed as described in Fig. 1d. **f)** Complementation of the MSD2 domain processing. MSD2 was coexpressed with the indicated M1 containing construct. Processing of the M2 was analysed by immunoblotting (*top panel*) and cell surface anti-HA Ab binding (*bottom panel*). **g)** MSD2-3HA containing domain combinations failed to undergo complex-glycosylation. M2, RM2, M2N2, RM2N2 and N1RM2N2 were expressed in COS7 cells and detected by immunoblotting with anti-HA Ab. Dashed line indicates complex-glycosylated wt CFTR.

Supplemental Figure 5. Mutagenesis of RXR motives fails to revert the biosynthetic processing defect of the M1 and M1N1 fragments.

a) Expression of indicated EGFP N-terminal fusion constructs were detected by immunoblotting with the MM13-4 anti-CFTR Ab. Abbreviations: M1-RK, MSD1-R29K; M1N1-3RK, MSD1-NBD1-R29K/R516K/R555K. **b)** M1-RK and M1N1-3RK was, predominantly, retained in the ER and failed to reach the plasma membrane, according to co-localization with Alexa594-WGA and CNX.

Supplemental Figure 6. Characterization of the CFTR four-domain folding unit (CFTR-1218X).

a) Protease susceptibility of the wt and truncated CFTR. Microsomes from BHK cell lines stably expressing 823X- (M1N1R), 1158X-, 1218X- and wt-CFTR were subject to limited proteolysis at the indicated concentration of chymotrypsin. Proteins were separated and immunoblotted with the L12B4 NBD1-specific anti-CFTR Ab. **b)** CFTR-1218X functions as halide selective channel in the presence of PKA and genistein stimulation. BHK cells, stably expressing the CFTR-1218X were loaded with sodium iodide. Iodide efflux into the extracellular medium was detected by iodide sensitive electrode. *Left panel*; genistein (50 μ M,

empty arrow head) and PKA activating cocktail (filled arrow head) addition as indicated. *Right panel:* PKA activating cocktail was added alone or with genistein. **c)** The effect of progressive C-terminal truncations of the MSD2 on CFTR expression. Schematic location of CFTR truncations (*top panel*). CFTR variants were transiently expressed in COS7 cells and equal amounts of proteins were immunoblotted with anti-HA Ab (*middle panel*). Cell surface density of CFTR variants was measured by the immunoperoxidase assay (*lower panel*). **d)** Immunolocalization of CFTR truncations in transiently transfected COS7 cells. Co-localization of CFTR with Alexa594-WGA and calnexin (CNX) was accomplished as described in Fig. 1d. **e)** Physical association of the split four-domain folding unit. M1 and N1RM2 were expressed alone or together in COS7 cells. Cell lysates were immunoprecipitated with polyclonal anti-CFTR NBD1-R Ab. Precipitates and lysates were probed with anti-HA and N-terminal specific anti-CFTR MM13-4 Ab. **f)** The stability and recovery efficiency of mature CFTR and CFTR-1218X are unaltered in ATP-depleted cells. CFTR or CFTR-1218X were metabolically labeled with ^{35}S -Met and ^{35}S -Cys for 10 min and chased for 3 hours to allow conformational maturation in the presence or absence of BFA. Then the cells were ATP-depleted with 10 μM CCCP, 10 mM deoxy-D-glucose and 4 $\mu\text{g/ml}$ Antimycin A for an additional 3 hours. CFTR was isolated by immunoprecipitation and visualized by fluorography.

Supplemental Figure 7. Probing the global and domain-wise conformational stability of CFTR mutants with limited proteolysis.

Microsomes were isolated from BHK cells expressing the indicated mutant and digested with increasing chymotrypsin concentration as described in Method. Polypeptides were separated by SDS-PAGE and probed by immunoblotting with a) N-terminal (MM13-4), b) NBD1 (660) and c) NBD2 (M3A7) specific Ab.

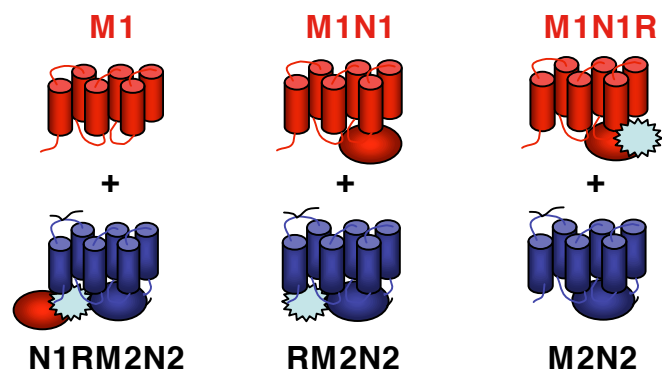
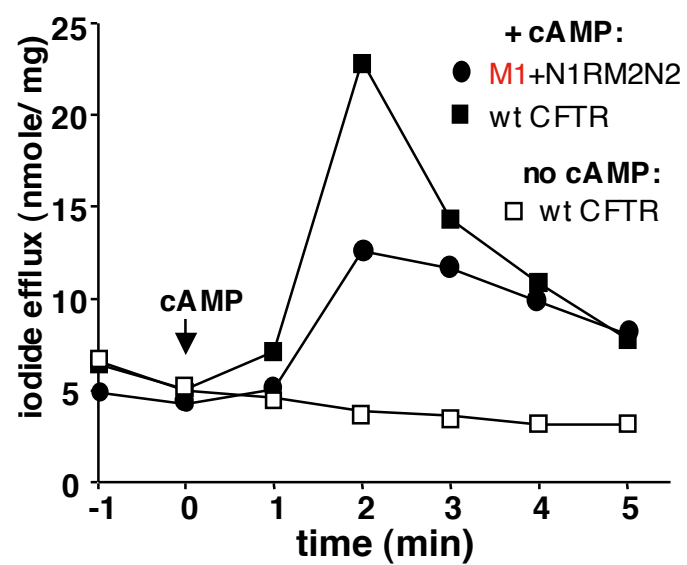
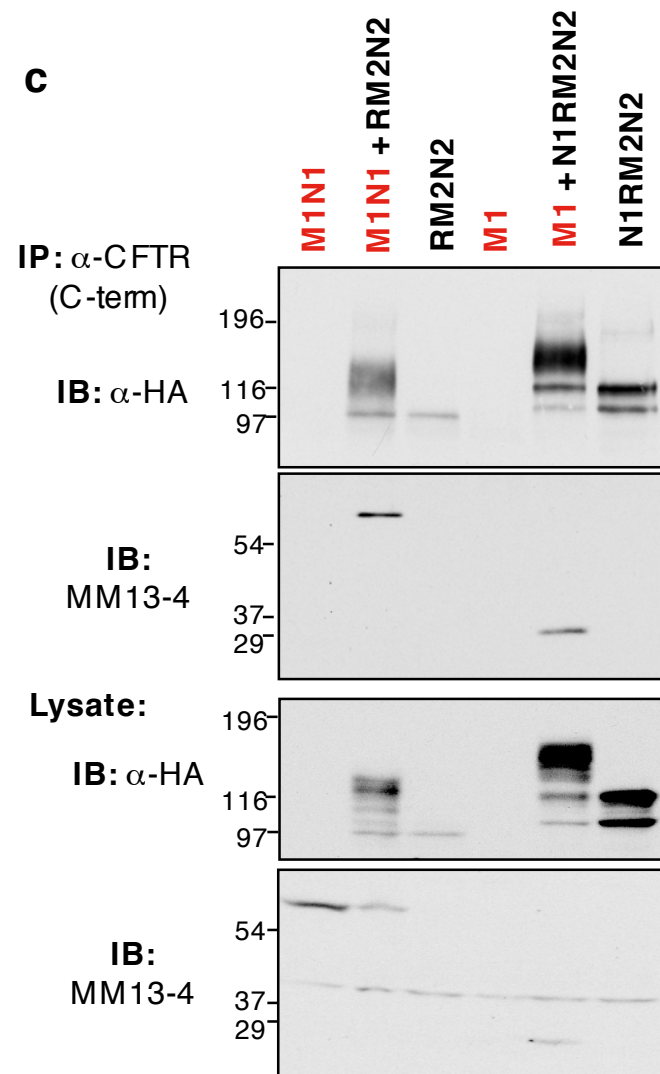
Supplemental Figure 8 Deletion of the NBD2 prevents the low temperature rescue of the ΔF508 CFTR-1218X.

BHK cells, stably expressing the ΔF508 CFTR the ΔF508 CFTR-1218X, were rescued for

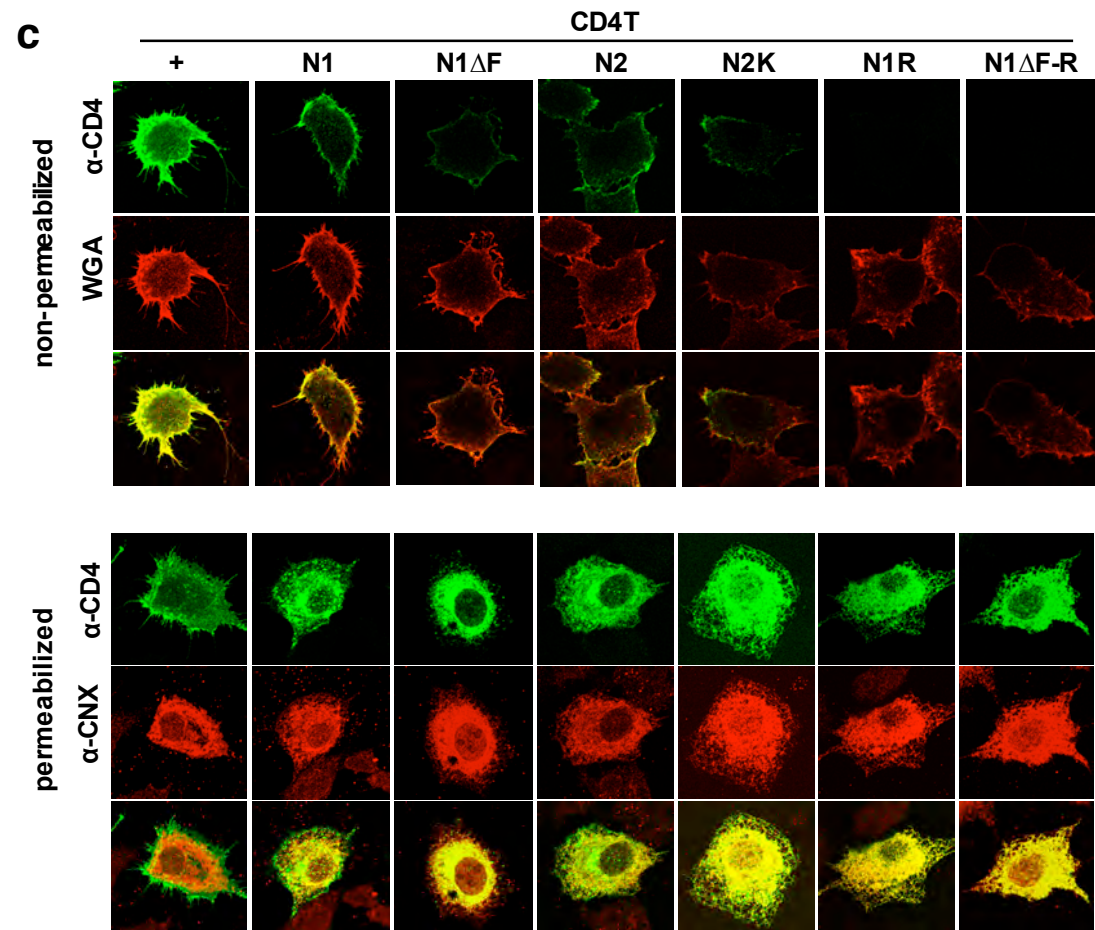
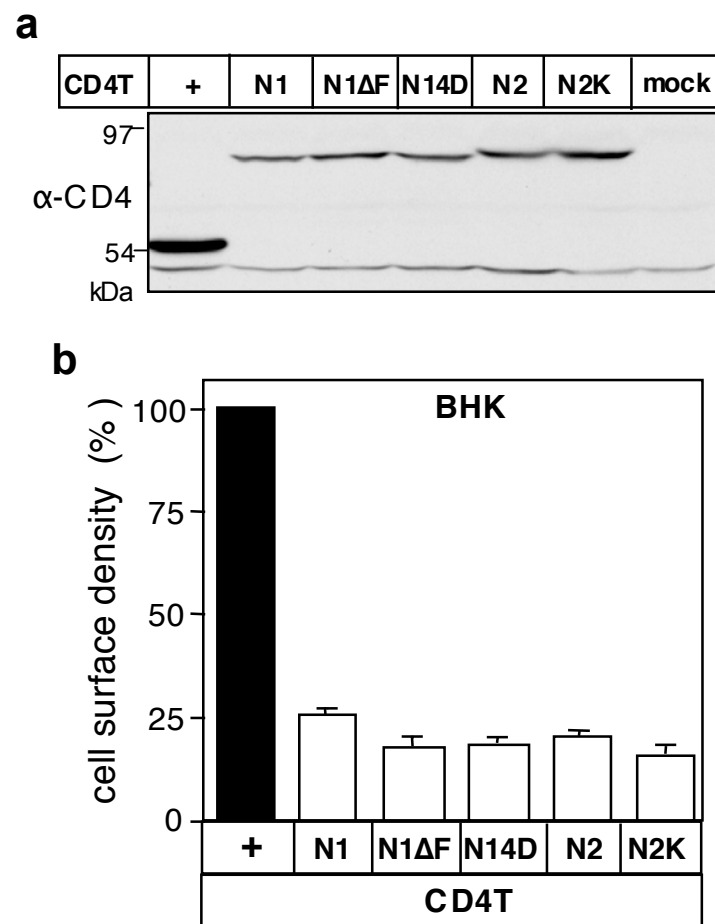
24h at 26°C in the presence of 10% glycerol. Processing of the mutant CFTRs was monitored by immunoblotting (*top panel*) and cell surface anti-HA Ab binding (*bottom panel*). The relative cell surface expression of CFTR constructs was expressed.

Supplementary Table

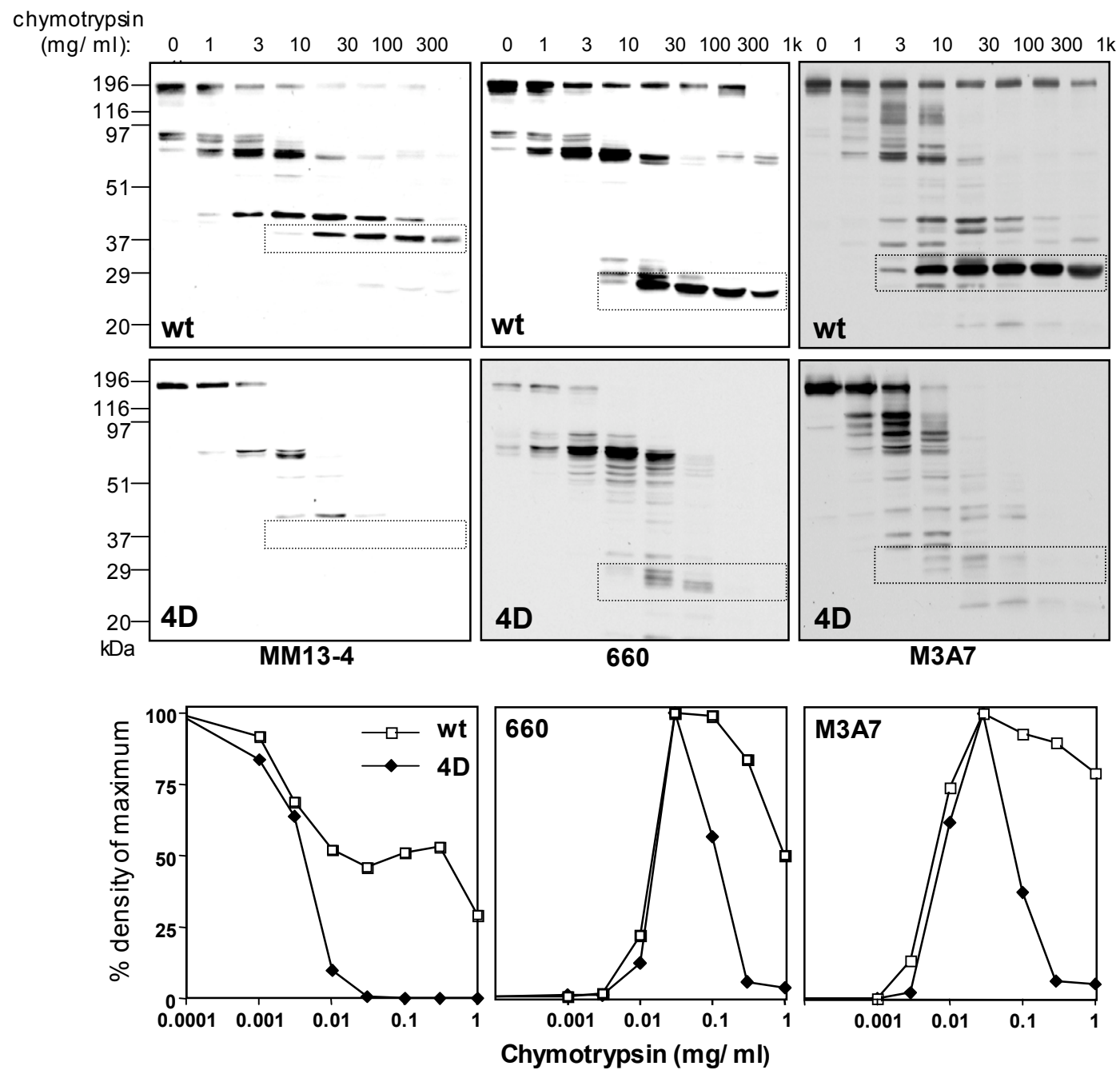
Domain	a.a. boundary	predicted M.W.
N-terminal fragments		
M1	1-414	48
M1*	1-388	45
M1N1	1-636	73
M1*N1	1-678	77
M1N1R	1-823	94
myc-M1N1	2-636	74
myc-M1N1R	2-823	95
GFP-M1	2-414	75
GFP-M1N1	2-636	100
GFP-M1N1R	2-823	121
C-terminal fragments		
M2	733-1218	54
M2#	837-1156	36
M2##	837-1218	43
RM2	634-1218	66
M2-N2	837-1480	73
RM2N2	634-1480	96
R*M2N2	679-1480	91
N1RM2N2	433-1480	118
N1*RM2N2	389-1480	123
N1RM2	351-1218	98
C-terminal truncations		
CFTR-1041X	1-1041	120
CFTR-1097X	1-1097	125
CFTR-1128X	1-1128	129
CFTR-1158X	1-1158	132
CFTR-1174X	1-1174	134
CFTR-1197X	1-1197	136
CFTR-1218X	1-1218	138
cytosolic domains		
CD4T-N1	351-636	80
CD4T-N1ΔF	351-636	80
CD4T-N14D	351-636	80
CD4T-N1*	389-678	79
CD4T-N1*ΔF	389-678	79
CD4T-N1*4D	389-678	79
CD4T-N2	1152-1480	84
CD4T-N2K	1152-1480	84
CD4T-R	679-836	68
R-liT	679-836	56
CD4T-N1R & mutants	351-823	102

a**b****c**

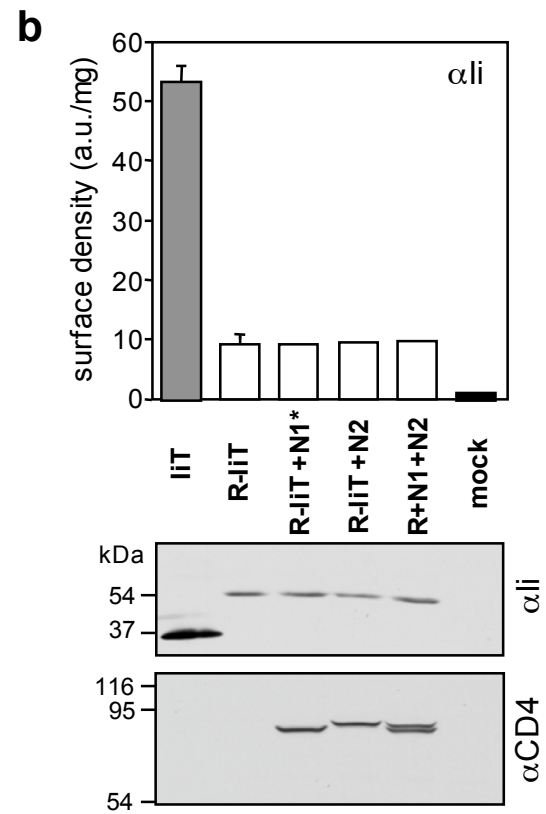
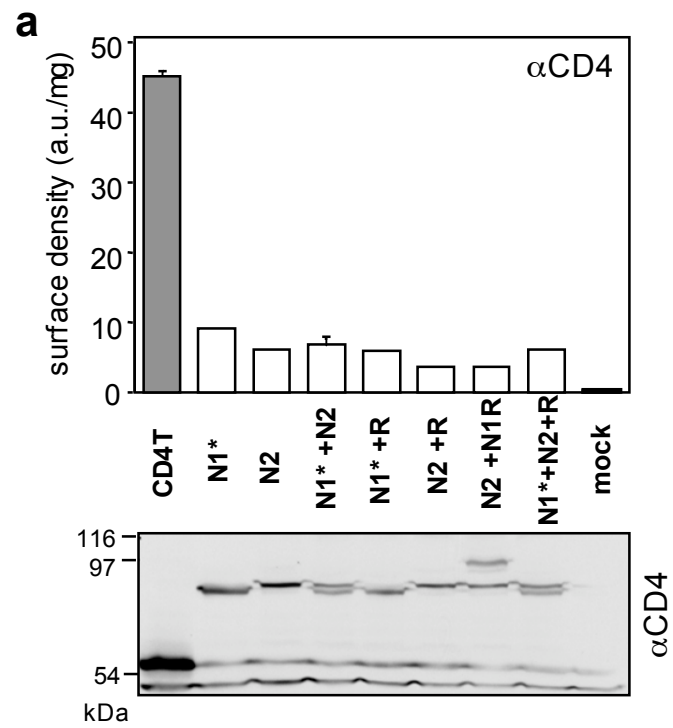
Supplemental Fig. 1.



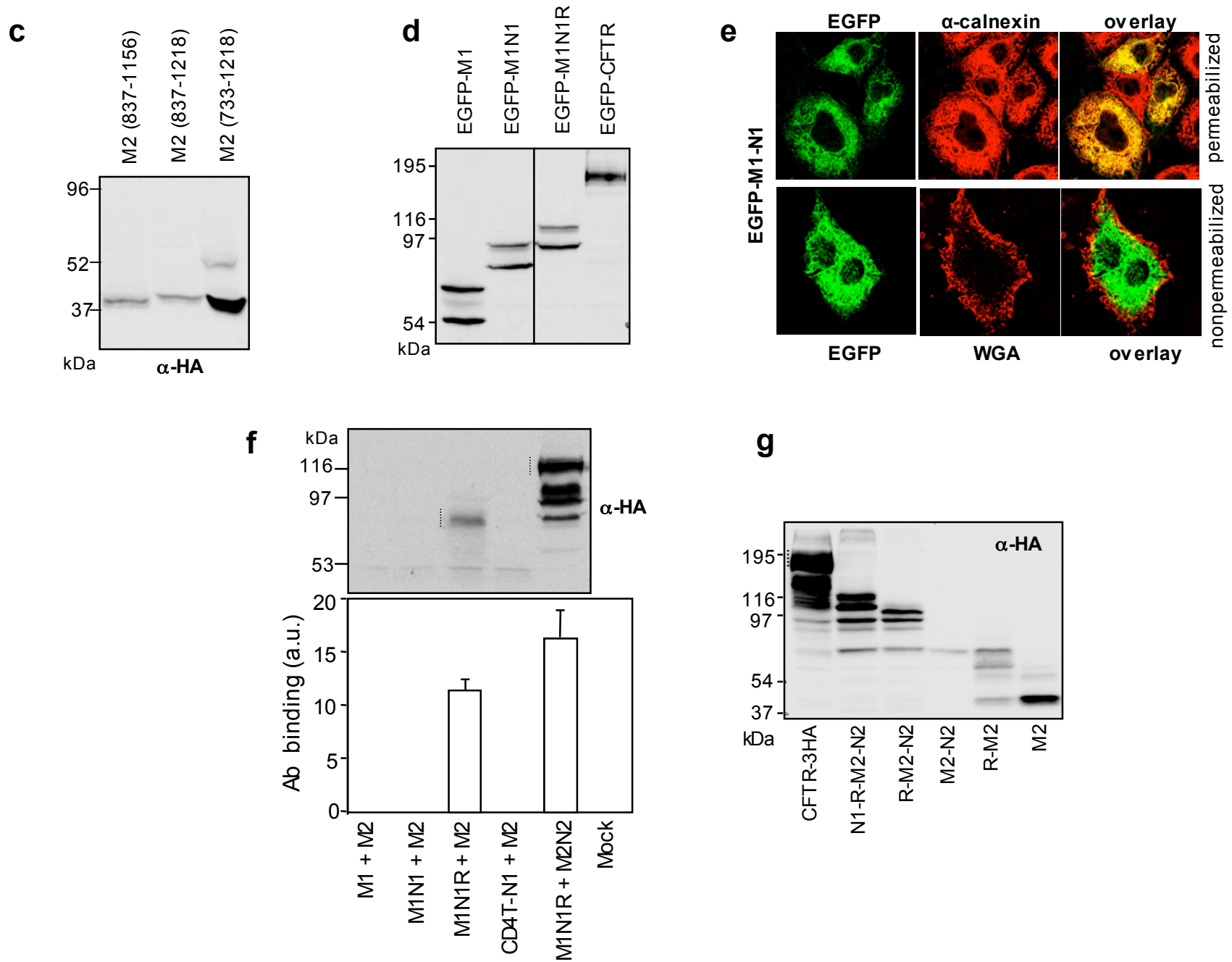
Supplemental Fig. 2.



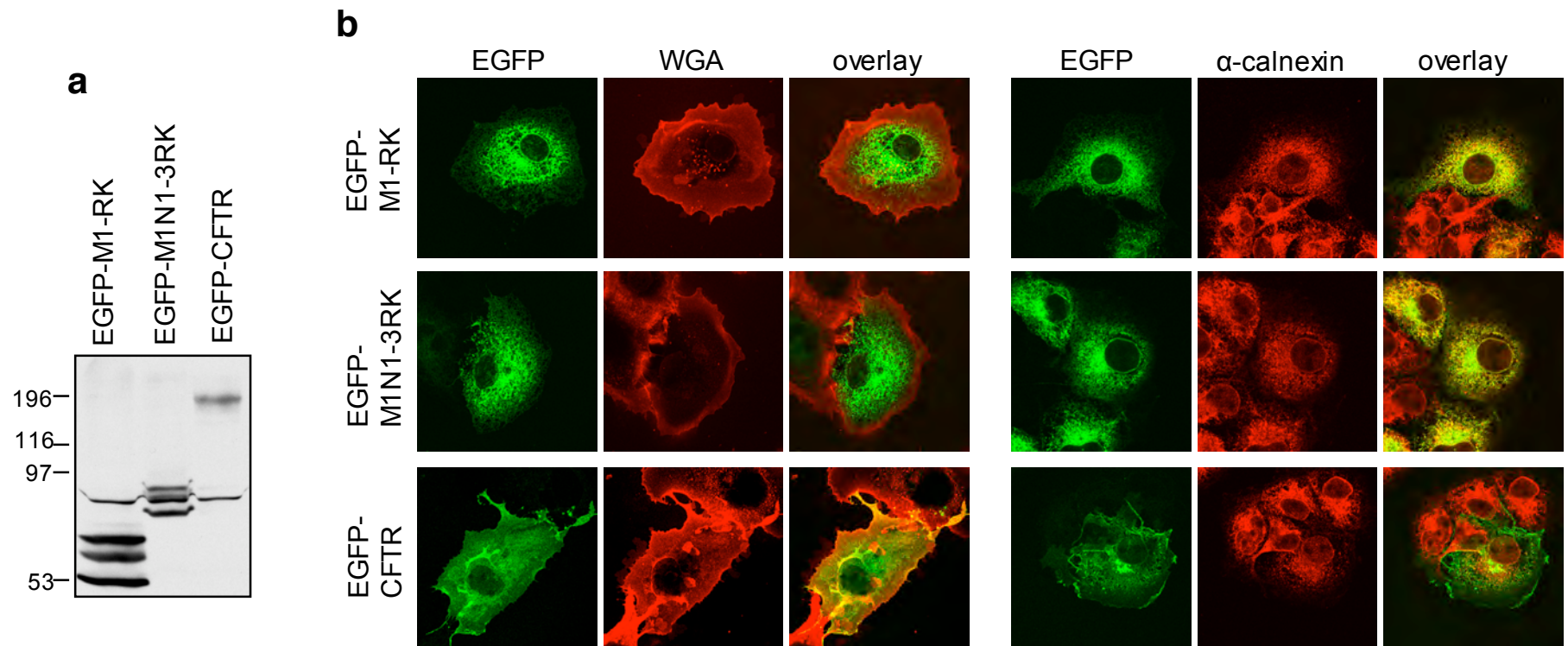
Supplemental Fig. 3.



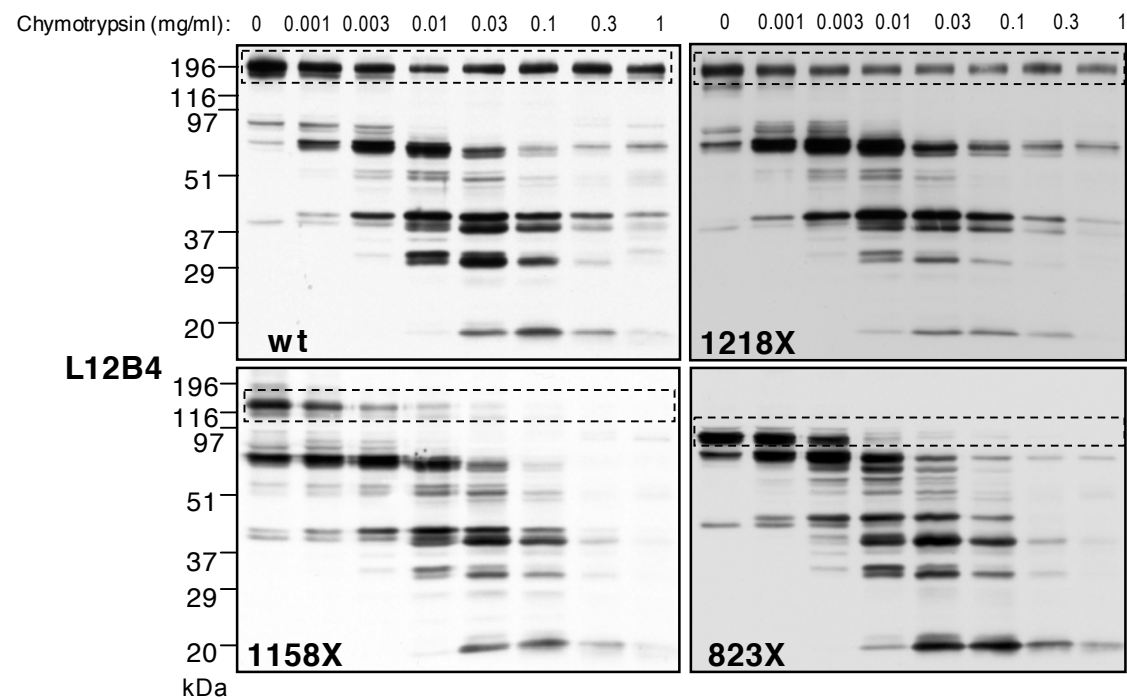
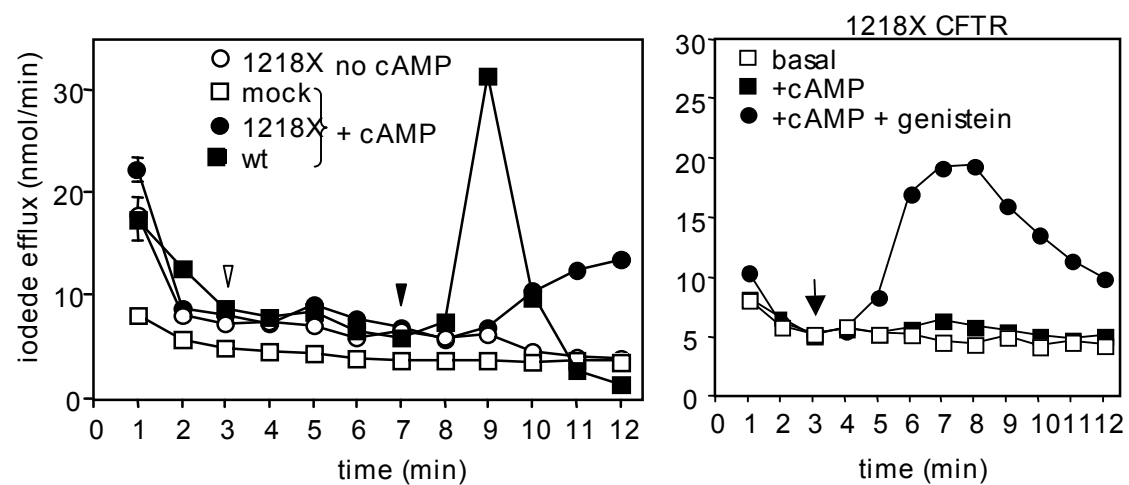
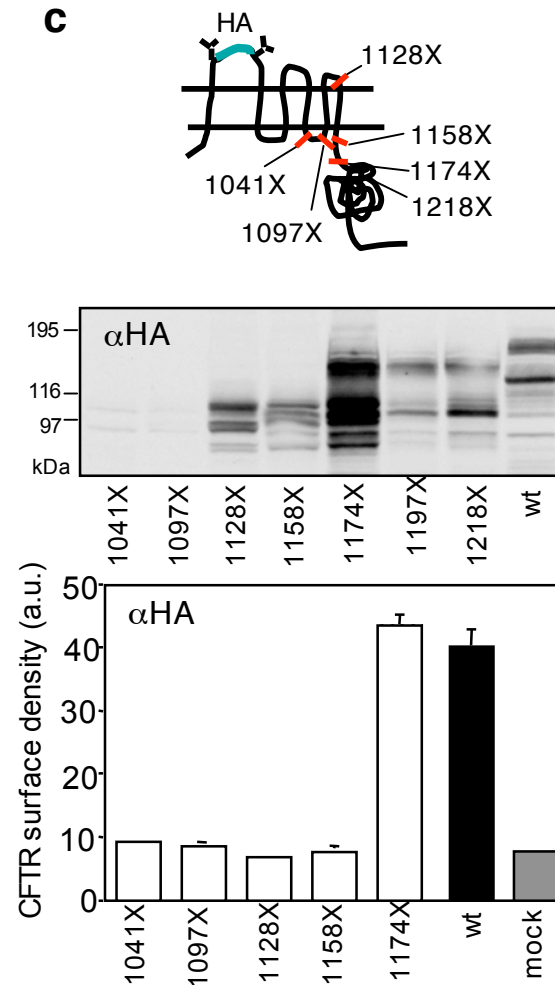
Supplemental Fig. 4.

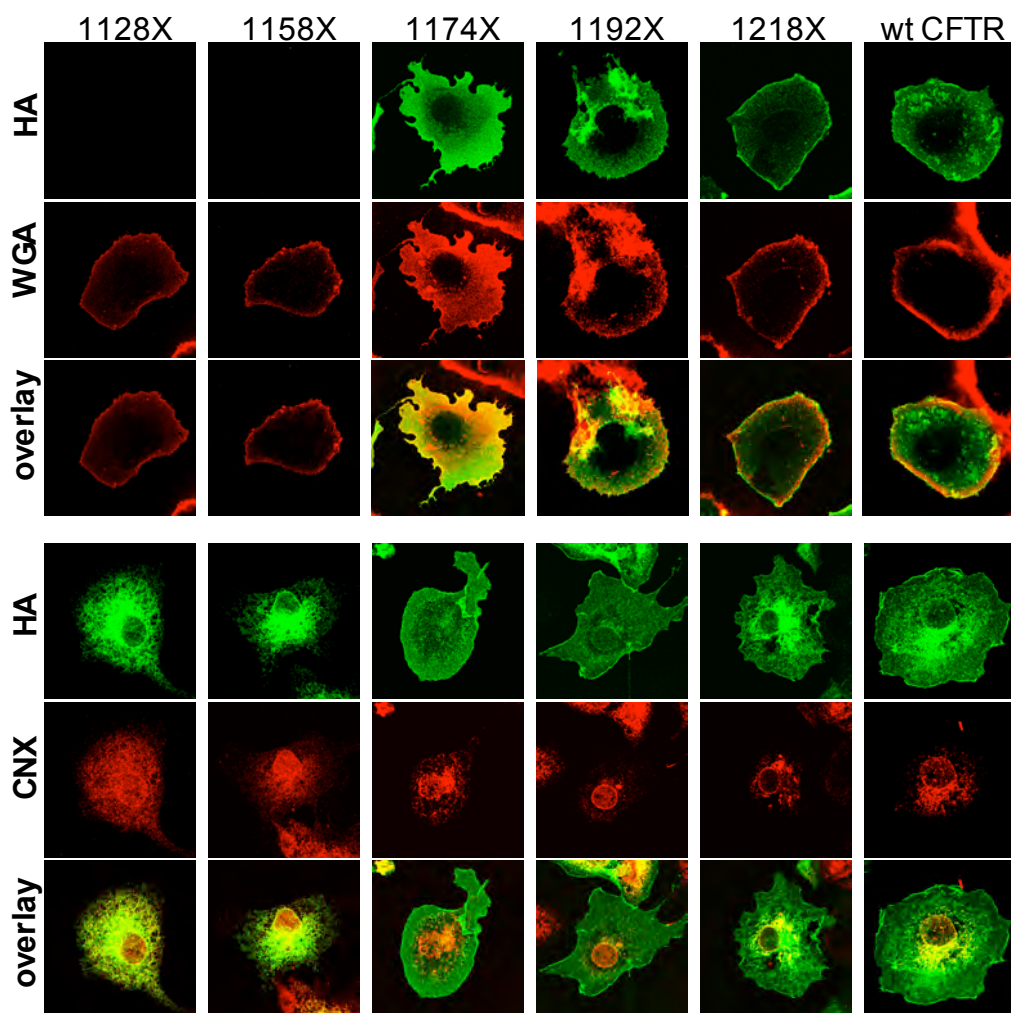
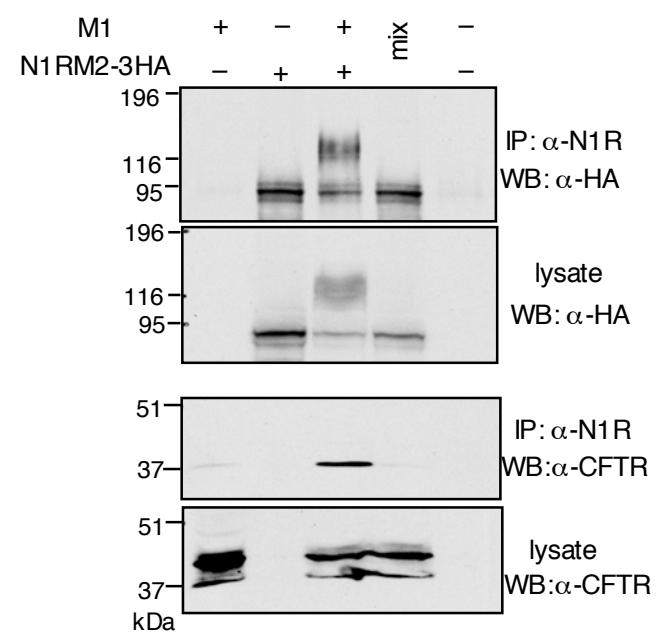
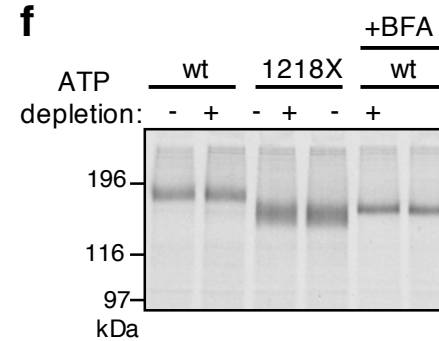


Supplemental Fig. 4.



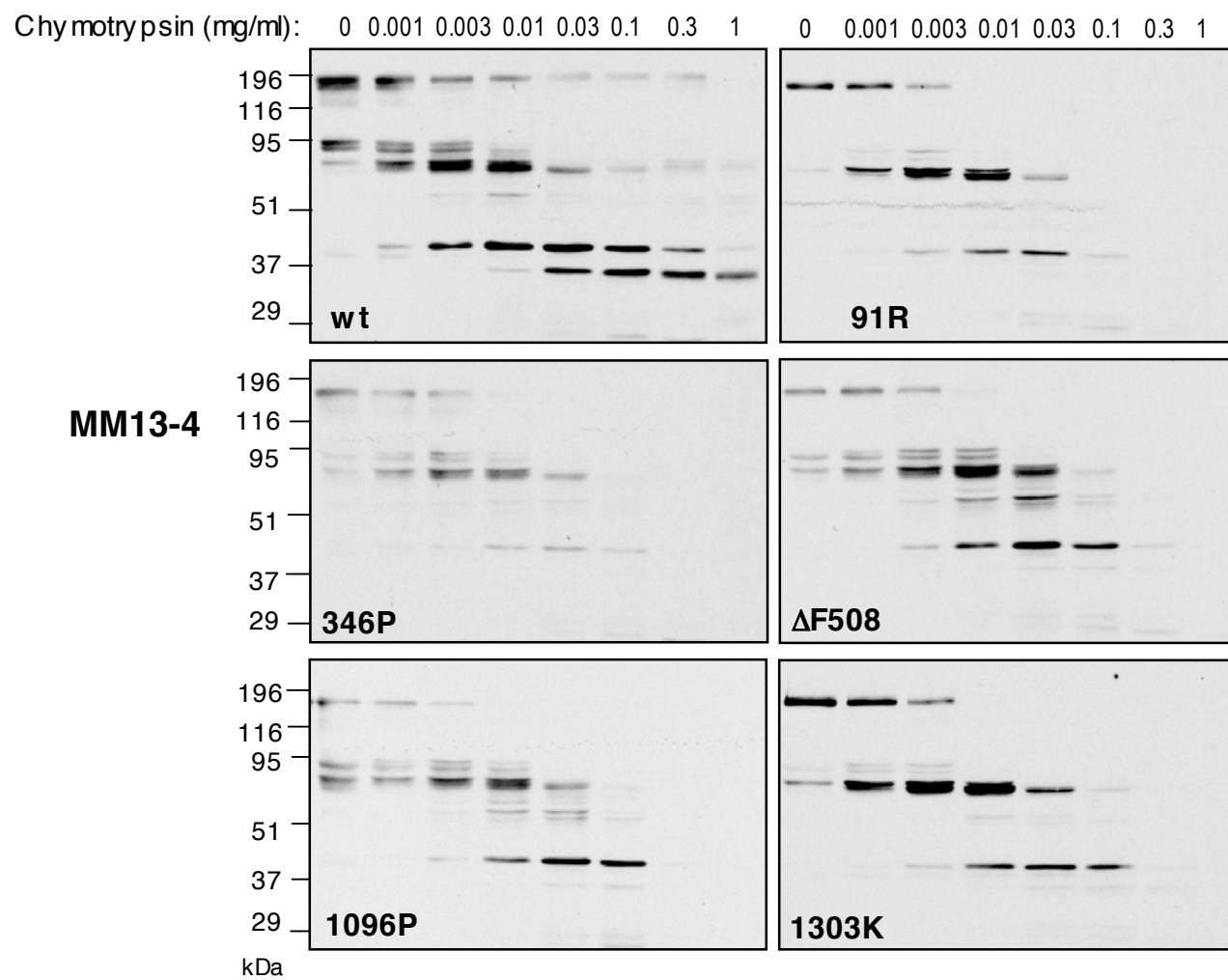
Supplemental Fig. 5.

a**b****c****Supplemental Fig. 6.**

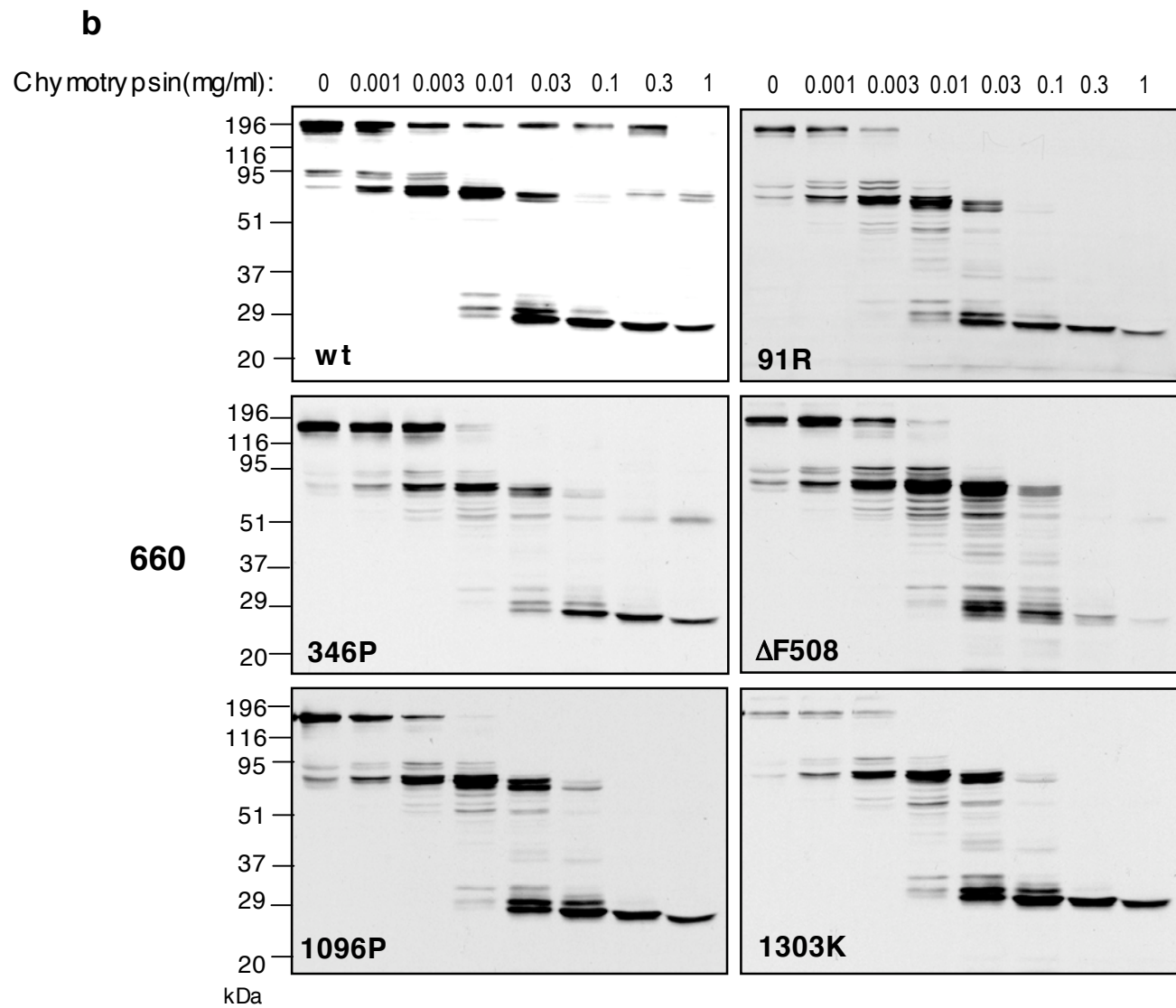
d**e****f**

Supplemental Fig. 6.

a

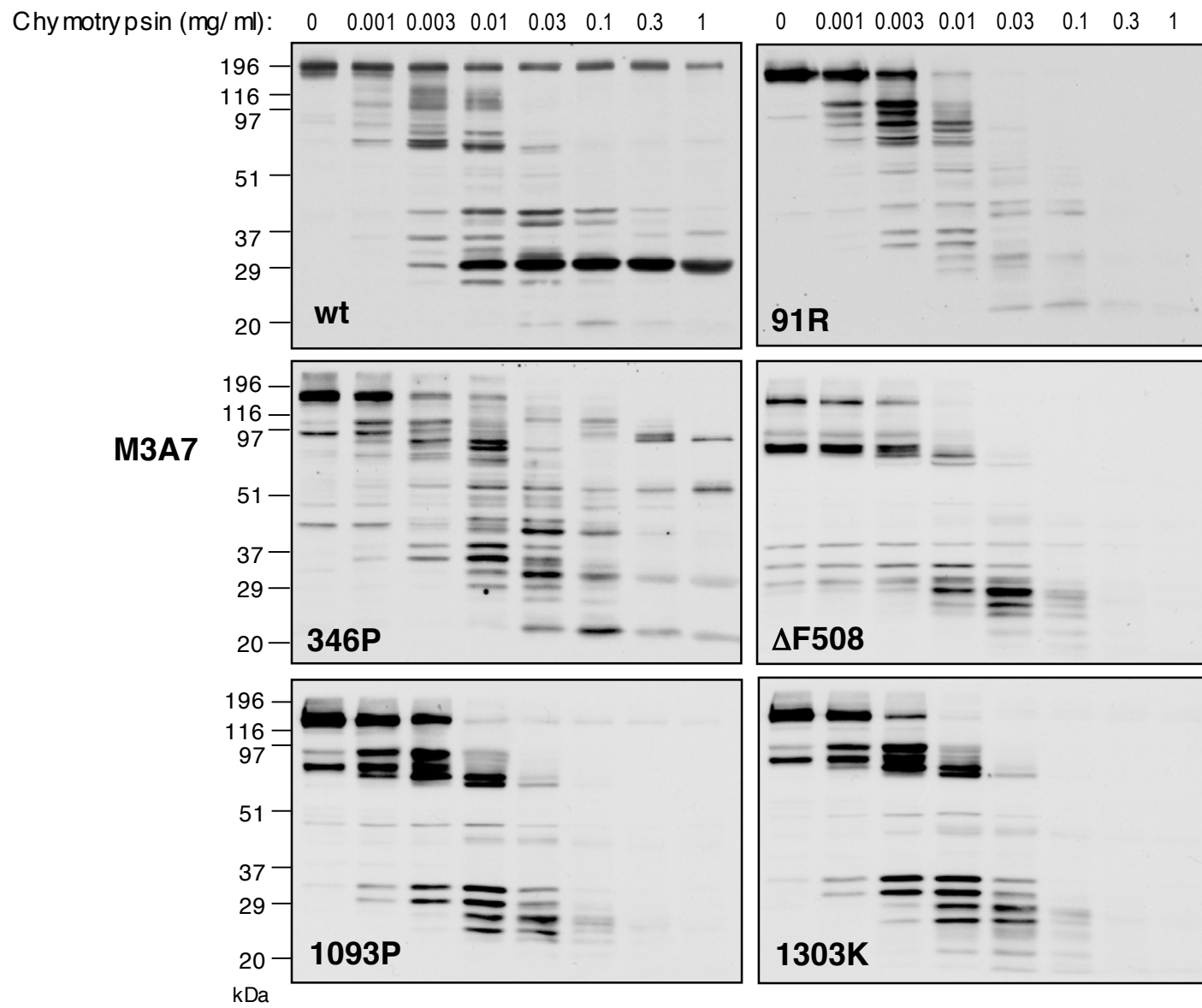


Supplemental Fig. 7.

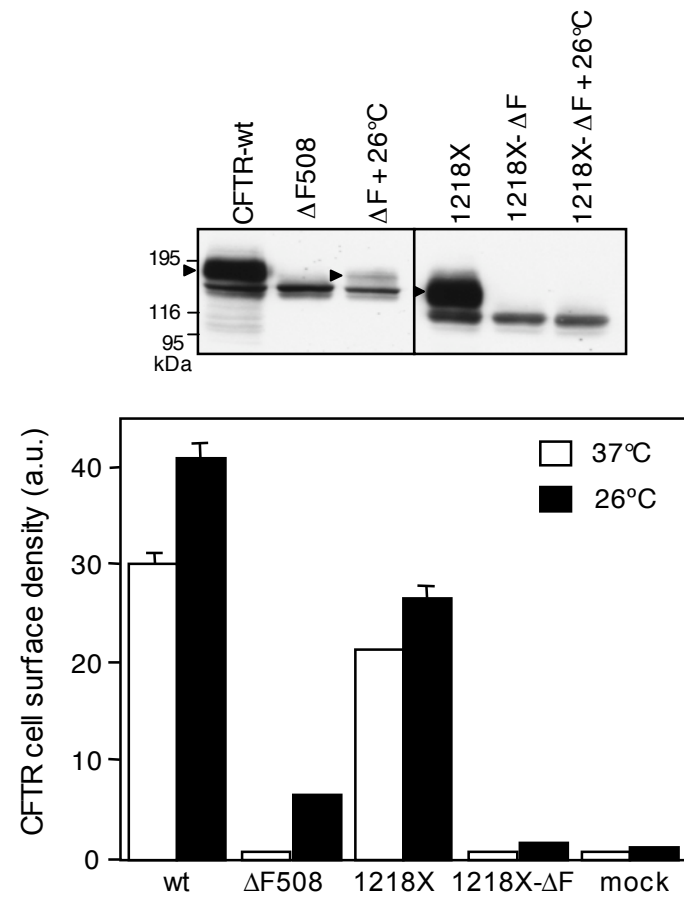


Supplemental Fig. 7.

c



Supplemental Fig. 7.



Supplemental Fig. 8.